mining

MDPI

Article

Verification Method and Engineering Practice for the Operational Characteristics of Paste–Solid Composite Backfilling Hydraulic Supports

Guochuan Zhang [1], Zishan Jin [2,3,*], Mao Li [1], Qiang Zhang [2], Tairan Han [1], Yuanzhi Zhang [4] and Ruiyi Zhang [2]

[1] China Pingmei Shenma Holding Group Co., Ltd., Pingdingshan 467000, China
[2] School of Mines, China University of Mining & Technology, Xuzhou 221116, China; leafkky@163.com (Q.Z.); ruiyi0323@163.com (R.Z.)
[3] School of Energy, China University of Mining & Technology, Xuzhou 221116, China
[4] Pingdingshan Tianan Coal Industry Co., Ltd., Pingdingshan 467000, China
* Correspondence: jinzsh@163.com; Tel.: +86-15503783173

Abstract

Coal mine backfilling mining technology has developed rapidly in recent years. Composite backfilling technology, which integrates two single backfilling methods, is an approach that achieves multiple engineering objectives, including improved backfilling efficiency, enhanced stability of the backfilling body, effective control of surface deformation, reduced backfilling costs, and rational disposal of solid waste. As the core equipment of composite backfilling technology, the paste–solid composite backfilling hydraulic support is key to achieving the coordinated injection of both slurry and bulk materials in the composite backfilling working face. Verification of its operational characteristics is therefore necessary to ensure that the support meets the requirements for roof support and rear-area backfilling. This paper establishes an indicator system for the operational characteristics of the paste–solid composite backfilling hydraulic support and proposes assessment methods for six characteristic categories: structural, support, load-bearing, sealing, spatial compatibility, and backfilling coordination. For the Ji16-17-24100 working face at Pingmei No. 11 Coal Mine, the ZC13000/30/65D support was selected with a rated working resistance of 13,000 kN. The selected side-throwing belt speed is 3.5 m/s, within the calculated admissible range of 0–5.48 m/s, and the maximum allowable conveying resistance of the suspended belt is 33,640 N. The case study is a design-stage assessment under the specified engineering conditions; field performance should be evaluated using monitoring data.

Keywords: composite backfilling mining; backfilling hydraulic support; operational characteristics; verification method; engineering practice

Check for updates

Academic Editor: Shuai Cao

Received: 13 September 2026
Revised: 21 October 2026
Accepted: 26 October 2026
Published: 28 October 2026

Copyright: © 2026 by the authors. Licensee MDPI, Basel, Switzerland. This article is an open access article distributed under the terms and conditions of the Creative Commons Attribution (CC BY) license.

1. Introduction

Coal will continue to occupy a dominant position in China's energy structure in the short term, playing a fundamental role in ensuring national energy security and supporting the stable development of renewable energy systems [1–3]. However, the sustainable development of the coal industry is significantly constrained by coal extraction beneath buildings, water bodies, and railways (collectively referred to as "three-under" coal resources) and the disposal of coal-based solid wastes. To address the challenges associated with resource losses and gangue accumulation, backfilling mining technology has been extensively promoted and has achieved considerable progress in recent years [4,5]. By utilizing underground goafs for the disposal of coal gangue, backfilling coal mining can

effectively reduce solid waste emissions, mitigate mining-induced subsidence hazards, and improve resource recovery efficiency, making it one of the key technologies for realizing green and sustainable coal mining [6,7].

In recent years, extensive theoretical investigations and engineering practices have been conducted on backfilling mining modes and associated key technologies. Regarding the innovation of backfilling mining modes, Xie et al. [8] proposed the concept of negative-carbon and high-efficiency backfilling mining, in which a highly porous solid framework formed by gangue and cementitious materials was employed for stable CO_2 storage. Zhang et al. [9] developed a four-element coal resource development model and established an integrated underground production system involving excavation, mining, separation, and backfilling processes. Zhang et al. [10,11] proposed the concept of fully mechanized top-coal caving backfilling mining and a three-dimensional backfilling strategy involving the combined application of multiple backfilling technologies to fill mining-induced cavities at different strata levels within the overburden system. Zhu et al. [12] integrated geological CO_2 sequestration technology with coal mine backfilling technology and proposed an interval-strip backfilling method for CO_2 mineral sequestration in underground goafs, together with its key technical approaches. Zhang et al. [13] proposed a gaseous CO_2 sequestration mode within strip mining goafs and experimentally investigated the impermeability performance of surrounding sealing walls designed to prevent horizontal migration of CO_2 gas. Deng et al. [14] introduced microbial-induced calcium carbonate precipitation (MICP) technology into backfilling mining and developed a microbial-induced calcium carbonate precipitation cemented backfilling technology for coal mines. Zhang et al. [15] proposed a shortwall cemented backfilling method for coal pillar recovery based on the concept of "temporal coordination–coal pillar replacement". Furthermore, several researchers have proposed technologies for the coordinated development of geothermal energy and coal resources in deep mines [16], including energy-storage backfilling technology and phase-change heat-storage functional backfilling technology [17].

Regarding key technologies associated with backfilling mining, Yang et al. [18] investigated the slurry formation mechanism of coal-based solid waste backfilling materials, steady-state flow control of backfilling slurry, and the evolution characteristics of pore structures within backfilled materials. Lyu et al. [19] proposed the scientific concept of a "coal underground space responsive enhanced thermal storage backfilling system" based on the concept of functional backfilling. Chang et al. [20] established a mechanical model of a dynamic heterogeneous composite elastic foundation beam for the roof structure and revealed the collaborative load-bearing mechanism between multilayer backfilled bodies and surrounding rocks in deep thick coal seams. Liu et al. [21] established calculation methods for working face support strength and overburden deformation control equations under three backfilling engineering modes: ecological environmental protection, surface building protection, and gangue solid waste disposal. Wang et al. [22] analyzed the influence of the aeolian sand replacement ratio (the mass ratio of aeolian sand replacing gangue) on the mechanical properties of gangue–aeolian sand cemented backfilling materials. Li et al. [23] revealed the coupled interaction mechanism between supports and surrounding rocks in thick top-coal backfilling faces and proposed an optimization method for support parameters.

Overall, existing studies on coal mine backfilling mainly focus on paste backfilling, solid backfilling, and cemented backfilling technologies, with backfilling materials primarily consisting of coal-based solid waste slurry and granular solid materials. However, research on paste–solid composite backfilling technology remains at an early stage [24]. As the core equipment of paste–solid composite backfilling technology, the paste–solid composite backfilling hydraulic support is central to achieving coordinated transportation and injection

of slurry and granular materials in combined backfilling working faces. Verification of its operational characteristics is therefore required to ensure its adaptability for both roof support and rear-area backfilling operations.

This paper establishes an evaluation index system for the operational characteristics of paste–solid composite backfilling hydraulic supports and proposes verification methods for six characteristic categories. A case study is conducted to examine the applicability of these methods to support selection and design under specified geological and operating conditions. An engineering case is used here to assess whether the proposed methods support selection and design under the specified geological and operating conditions.

2. Paste–Solid Composite Backfilling Hydraulic Support and Operational Characteristics Evaluation Framework

2.1. Structural Composition and Functions of the Paste–Solid Composite Backfilling Hydraulic Support

Here, "paste–solid composite backfilling" refers to a method in which paste slurry and granular coal gangue are placed in a coordinated sequence or operation to form a composite backfilled body. A "paste–solid composite backfilling hydraulic support" is a support equipped to accommodate both paste–slurry injection and granular-gangue placement. The paste–solid composite backfilling hydraulic support integrates the functions of paste–slurry injection and granular-gangue placement. It is developed through structural modification of the mechanical body of a conventional paste backfilling hydraulic support and incorporates two independent backfilling mechanisms for paste slurry and gangue particles. Specifically, a suspended gangue-throwing belt conveyor and a side-throwing belt conveyor are installed on the rear top beam of the paste backfilling hydraulic support.

The filling pipeline suspended beneath the rear top beam is used for injecting paste slurry into the goaf. Meanwhile, a rear sliding rail system is installed to support the suspended gangue-throwing belt conveyor, which transports granular gangue materials, while the side-throwing belt conveyor transfers and disperses gangue particles into the goaf. Figure 1 shows the support structure.

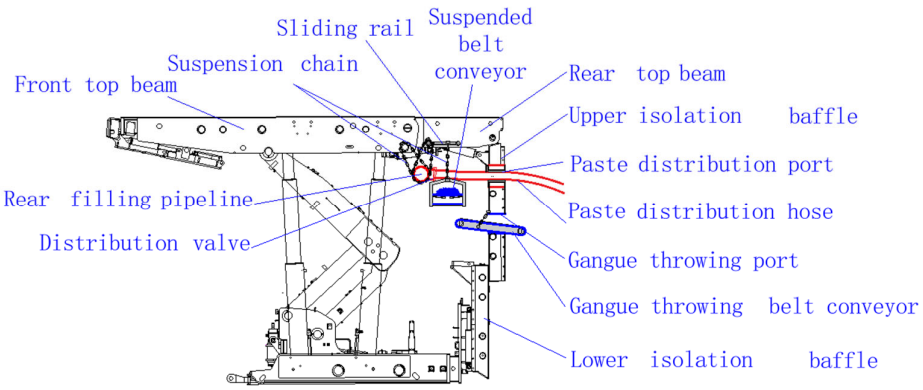


Figure 1. Mechanical structure of paste–solid composite backfilling hydraulic support.

The backfilling process of the paste–solid composite backfilling hydraulic support consists of three sequential stages. First, paste slurry is injected behind the support until a predetermined filling height is reached. Subsequently, granular gangue materials are transported through the suspended gangue-throwing belt conveyor and the side-throwing belt conveyor into the goaf, where they are simultaneously placed to achieve the designed filling height. Finally, the gangue-throwing belt conveyor is withdrawn, the gangue discharge opening is closed, and paste slurry is further injected to achieve dense roof-contact

backfilling. Under the action of gravity, gangue particles gradually settle and become immersed in the paste slurry. After solidification, the paste–solid composite backfilled body forms an integrated load-bearing structure, which jointly supports the overlying roof strata.

2.2. Operational Characteristics Evaluation Framework of the Hydraulic Support

The operational characteristics of the paste–solid composite backfilling hydraulic support refer to its overall capability to protect the backfilling space, provide transport pathways for backfilling materials, seal the paste backfilling zone, and ensure the required filling ratio. The operational characteristics of the paste–solid composite backfilling hydraulic support mainly consist of six aspects: structural characteristics, support characteristics, load-bearing characteristics, sealing characteristics, spatial compatibility characteristics, and backfilling-coordination characteristics. These characteristics provide the fundamental basis for evaluating and determining the control performance and adaptability of backfilling hydraulic supports. The operational performance of backfilling hydraulic supports is mainly influenced by three factors: support configuration, geological conditions, and backfilling process. Among them, the support configuration directly determines the operational performance of the hydraulic support. Geological conditions, including coal seam thickness, roof and floor conditions, coal seam inclination, and mining depth, affect the performance of the backfilling support during operation.

The evaluation indicators of the operational characteristics of the backfilling hydraulic support include support configuration, support intensity, support resistance, initial supporting force, load-bearing characteristics, and the contact condition between the rear isolation baffle and the backfilled material. Specifically, structural parameters such as support configuration are classified as structural characteristics; support intensity, support resistance, and initial supporting force correspond to support characteristics; the overlap ratio and contact angle of the rear isolation baffle are defined as sealing characteristics; and the distances between the paste distribution pipeline and gangue-throwing belt conveyor, between the gangue-throwing belt conveyor and isolation baffle, and between the belt discharge center and filling area are categorized as spatial compatibility characteristics. Furthermore, the paste–solid filling matching degree and belt transfer efficiency are considered composite backfilling characteristics. Figure 2 presents the evaluation index system for these operational characteristics.

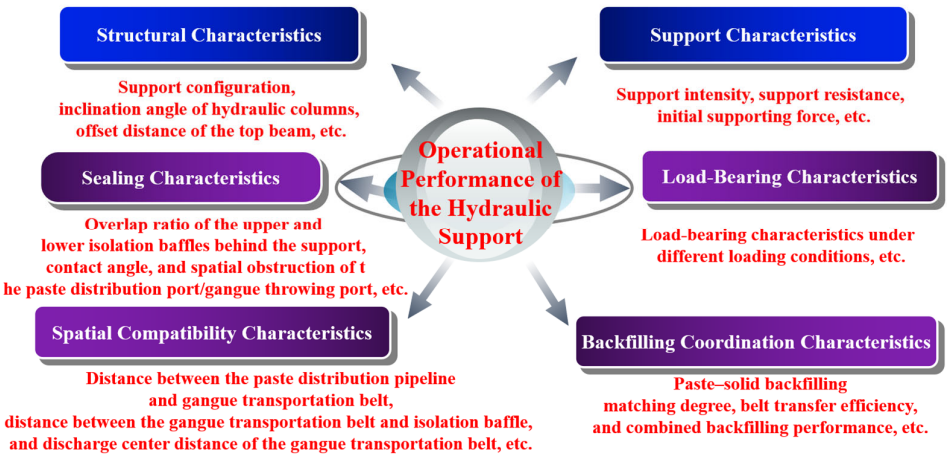


Figure 2. Operational characteristic indicator system for paste–solid composite backfilling hydraulic support.

3. Key Indicators and Verification Methods for the Operational Characteristics of the Hydraulic Support

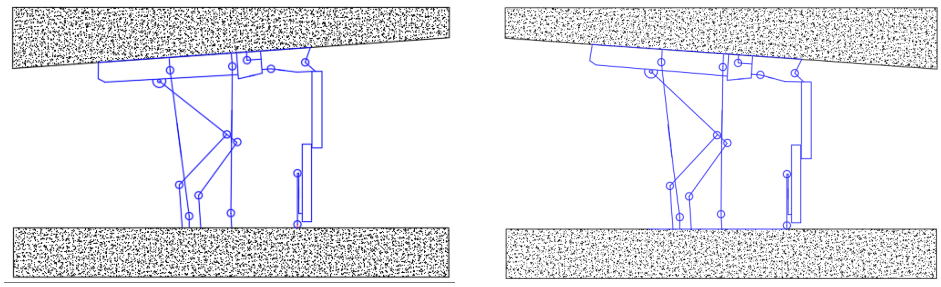
Since the mechanical body structure of the paste–solid composite backfilling hydraulic support is generally similar to that of conventional backfilling hydraulic supports, the relevant indicators associated with structural, support, and load-bearing indicators have been extensively investigated and reported in previous studies [25,26]. Therefore, this section focuses on several key sealing, spatial-compatibility, and backfilling-coordination indicators and their corresponding verification methods for the paste–solid composite backfilling hydraulic support.

3.1. Sealing Characteristics of the Paste–Solid Composite Backfilling Hydraulic Support

The rear movable isolation baffle of the paste–solid composite backfilling hydraulic support consists of an upper baffle and a lower baffle. The lower baffle is fixed on the base of the hydraulic support, whereas the upper baffle is hinged to the rear top beam and can move forward and backward using hydraulic cylinders. An insert plate is installed inside the upper baffle and can move in a way vertically driven by hydraulic cylinders. The insert plate compensates for the limited length of the upper baffle and forms an integrated sealing structure with the upper baffle, providing lateral restraint and support for the backfilled body. Meanwhile, in the paste–solid composite backfilling process, injection ports and gangue discharge ports are arranged on the upper baffle to facilitate paste–slurry injection and gangue backfilling operations, respectively.

1. Sealing Degree

Due to the unique structural characteristics and backfilling process of the large-mining-height paste–solid composite backfilling hydraulic support, deformation of the hydraulic support may occur under complex geological conditions during backfilling operations, resulting in two typical roof beam deformation states: the forward inclination ("head-down") state and the backward inclination ("head-up") state. Under these two conditions, the upper isolation baffle hinged to the rear top beam overlaps with the lower isolation baffle, forming a certain degree of sealing between the upper and lower isolation baffles, as shown in Figure 3.



(**a**) (**b**)

Figure 3. Schematic diagram of sealing performance: (**a**) Forward inclination condition of the top beam. (**b**) Backward inclination condition of the top beam.

The sealing degree is primarily determined by the height of the backfilling space. Under the applicable mining height conditions of the hydraulic support, the sealing degree varies with changes in the backfilling space height. To prevent deformation and leakage of the rear backfilling baffle under the maximum pressure exerted by the backfilled body, the sealing degree should be maintained within a reasonable range and remain higher than its minimum allowable value.

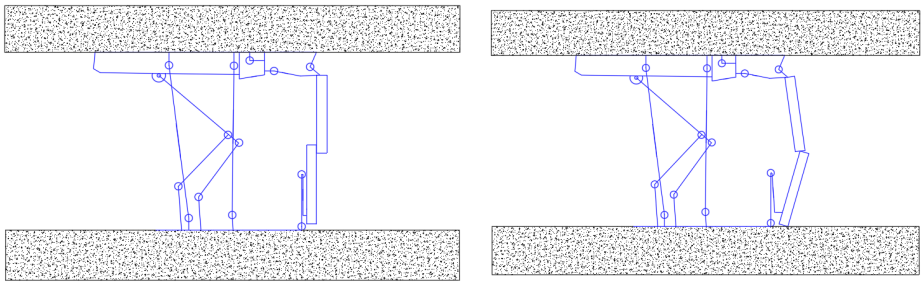
The actual overlap length between the upper and lower isolation baffles is denoted by H_{act}, and the minimum allowable overlap length is denoted by H_{min}. The sealing criterion is expressed as Equation (1):

$$H_{act} \geq H_{\text{min}} \quad (1)$$

where H_{act} is the actual overlap length between the upper and lower isolation baffles behind the hydraulic support, in meters, and H_{min} is the minimum allowable overlap length, in meters.

2. Contact Angle

The contact angle refers to the included angle between the upper and lower isolation baffles when they are in contact behind the hydraulic support. During the adjustment process, the upper isolation baffle cannot achieve complete surface contact with the lower isolation baffle due to structural constraints, resulting in a certain contact angle, as shown in Figure 4.



(**a**) (**b**)

Figure 4. Schematic diagram of contact angle: (**a**) Normal operating condition. (**b**) Contact angle formation condition.

The contact angle also influences the sealing degree of the isolation baffles. The actual contact angle is denoted by θ_{act}, and the critical contact angle corresponding to the specified non-leakage condition is denoted by θ_{crit}. The safety criterion is expressed as Equation (2):

$$\theta_{act} \leq \theta_{crit} \quad (2)$$

where θ_{act} is the actual included angle between the upper and lower isolation baffles, in degrees, and θ_{crit} is the critical angle corresponding to the specified non-leakage condition, in degrees.

3.2. Spatial Compatibility Characteristics

The spatial compatibility characteristics refer to the capability of the paste–solid composite backfilling hydraulic support to ensure that the suspended gangue-throwing belt conveyor and other components operate without interference after the belt conveyor is installed behind the support. During coal mining and gangue backfilling operations, the suspended gangue-throwing belt conveyor behind the hydraulic support may be affected by mining conditions such as upward and downward inclination of the working face. These changes may cause collision and interference between the belt conveyor, paste transportation pipelines, and rear structures of the hydraulic support. Continuous collision may damage the edge covering layer of the belt conveyor. Moreover, a significant increase in frictional resistance caused by mechanical interference may result in motor overload and shutdown. Severe collision-induced vibration may also cause gangue materials to spill from the edge of the conveyor, potentially injuring underground workers or damaging equipment, thereby affecting the normal operation of the gangue backfilling process. The

evaluation indicators of spatial compatibility characteristics mainly include the distance between the paste distribution pipeline and the suspended gangue-throwing belt conveyor, the distance between the suspended gangue-throwing belt conveyor and the isolation baffle, the discharge center distance of the suspended gangue-throwing belt conveyor, as well as geological factors such as coal seam thickness and roof and floor conditions.

Distance between the Paste Distribution Pipeline and Suspended Gangue-Throwing Belt Conveyor, Distance between Suspended Gangue-Throwing Belt Conveyor and Isolation Baffle, and Discharge Center Distance of the Suspended Gangue-Throwing Belt Conveyor.

During the operation of the hydraulic support, the distance between the paste distribution pipeline and the suspended gangue-throwing belt conveyor, the distance between the suspended gangue-throwing belt conveyor and the isolation baffle, and the discharge center distance of the suspended gangue-throwing belt conveyor vary continuously. Figure 5 defines these distances.

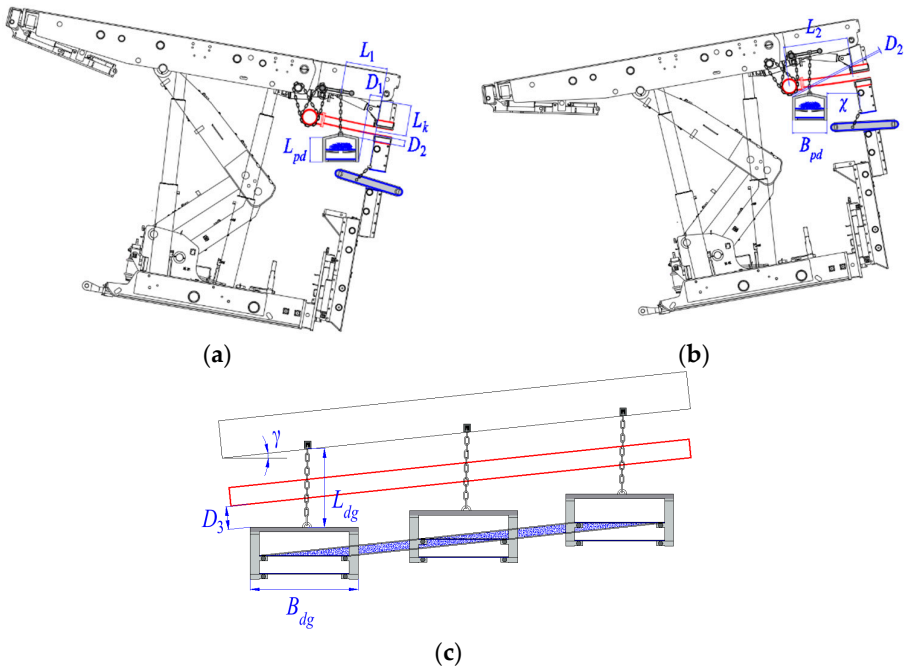


Figure 5. Schematic diagram of spatial compatibility characteristic indicators: (**a**) Upward inclination condition. (**b**) Downward inclination condition. (**c**) Rolling condition.

In the Figure 5, D_1 denotes the distance between the suspended gangue-throwing belt conveyor and the isolation baffle, mm; D_2 represents the distance between the longitudinal paste distribution pipeline and the suspended gangue-throwing belt conveyor, mm; L_1 denotes the distance from the suspension point of the suspended gangue-throwing belt conveyor to the inner side of the upper isolation baffle, mm; L_k represents the distance from the center of the paste distribution port to the bottom surface of the top beam, mm; L_{pd} denotes the length of the suspended gangue-throwing belt conveyor, mm; χ represents the discharge center distance of the suspended gangue-throwing belt conveyor, mm; L_2 denotes the distance from the suspension center of the paste distribution pipeline to the inner side of the upper isolation baffle, mm; B_{pd} represents the width of the suspended gangue-throwing belt conveyor, mm; D_3 denotes the transverse distance between the paste distribution pipeline and the suspended gangue-throwing belt conveyor, mm; γ represents the inclination angle of the working face, °; L_{dg} denotes the length of the suspension chain of the suspended gangue-throwing belt conveyor, mm; and B_{dg} represents the length of the suspended gangue-throwing belt conveyor, mm.

During the mining and backfilling operation of the hydraulic support, collision and interference among the gangue-throwing belt conveyor, isolation baffle, and paste distribution pipeline must be avoided. Therefore, the distances D_1, D_2, and D_3 between the suspended gangue-throwing belt conveyor and adjacent components should be greater than zero. The corresponding calculation criteria are given in Equations (3)–(6).

$$D_1 = L_1 - \frac{B_{pd}\cos\alpha_c}{2} - L_{pd}\sin\alpha_c - L_{dg}\sin\alpha_c > 0 \tag{3}$$

The inclination angle α_t of the paste distribution pipeline changes with the position of the paste distribution port opening. The corresponding calculation equation is expressed as follows:

$$\alpha_t = \alpha_c + \arctan\frac{L_k - H_{dg}}{L_2} \tag{4}$$

where α_c denotes the strike inclination angle of the working face, °.

Furthermore, based on the spatial geometric relationship, the calculation equation for the distance D_2 between the longitudinal paste distribution pipeline and the suspended gangue-throwing belt conveyor under upward and downward inclination conditions is derived as follows:

$$D_2 = L_{dg}\cos\alpha_t - H_{dg}\cos\alpha_t - (L_2 - L_1)\sin\alpha_t - d_t - \frac{B_{pd}\sin\alpha_t}{2} > 0 \tag{5}$$

where d_t denotes the diameter of the paste distribution pipeline, mm. Under the rolling condition of the hydraulic support, the spatial relationship between the transverse paste distribution pipeline and the suspended gangue-throwing belt conveyor changes accordingly. Based on the spatial geometric relationship, the calculation equation for D_3 is derived as follows:

$$D_3 = L_{dg}\cos\gamma - H_{dg} - \frac{L}{2}\sin\gamma - d_t > 0 \tag{6}$$

During gangue transfer from the suspended gangue-throwing belt conveyor to the side-throwing belt conveyor, the initial velocity of the gangue particles is considered to be zero. To ensure successful gangue discharge, the discharge center distance χ of the suspended gangue-throwing belt conveyor should remain positive. The corresponding verification equation is expressed as Equation (7).

$$\chi = L_1 - \frac{B_{pd}\cos\alpha_c}{2} + L_{dg}\sin\alpha_c > 0 \tag{7}$$

3.3. Backfilling Coordination Characteristics

During the backfilling operation, the paste–solid composite backfilling hydraulic support should possess sufficient coordination capability to ensure that paste slurry and gangue particles are injected into the goaf according to the required proportion. The corresponding evaluation indicators mainly include the paste–solid backfilling matching degree, belt transfer efficiency, side-throwing belt speed, and misalignment between the suspended gangue-throwing belt conveyor and its supporting frame.

1. Paste–solid Backfilling Matching Degree and Belt Transfer Efficiency

During the gangue backfilling process, granular gangue materials are transferred from the suspended gangue-throwing belt conveyor installed between adjacent hydraulic supports to the side-throwing belt conveyor and then discharged into the backfilling space. The conveying capacity of the side-throwing belt conveyor Q_{pg} should be greater than that of the suspended gangue-throwing belt conveyor Q_{pd}. Therefore, the belt transfer efficiency γ_z is defined as follows:

$$\gamma_z = \frac{Q_{pg}}{Q_{pd}} \tag{8}$$

The paste slurry is transported into the backfilling space through the paste distribution pipeline by an industrial pump. According to the designed paste-to-granular-gangue volume ratio in the composite backfilling process, the designed volume ratio of paste slurry to gangue materials is 1:1. The paste–granular backfilling matching degree σ_c is determined by the pumping velocity of the paste slurry and the conveying velocity of the belt conveyor, and the corresponding calculation equation is expressed as follows:

$$\sigma_c = \frac{3600 q_{pd} v_{pd}}{\rho_g Q_s} \tag{9}$$

where q_{pd} is the gangue load per unit length of the gangue-throwing belt conveyor, kg/m; v_{pd} is the conveying velocity of the gangue-throwing belt conveyor, m/s; and ρ_g is the density of gangue materials, kg/m^3.

2. Side-Throwing Belt Conveyor Velocity

To achieve uniform mixing of gangue materials and paste backfilled materials, the gangue particles should be distributed as much as possible in the middle region of the backfilling space. However, the falling position of gangue particles is closely related to the position of the side-throwing belt conveyor and the initial velocity of gangue particles. When the position of the side-throwing belt conveyor is fixed, an excessively low conveying velocity may cause the gangue particles to fall too close to the discharge point, whereas an excessively high velocity may result in collision with the rear backfilled body, leading to energy loss and unnecessary power consumption. Therefore, the velocity of the side-throwing belt conveyor should be maintained within a reasonable range.

In Figure 6, v_0 denotes the initial velocity of gangue particles discharged from the side-throwing belt conveyor, m/s; α_p represents the discharge angle of the side-throwing belt conveyor, °; H_p denotes the installation height of the side-throwing belt conveyor, m; and X represents the horizontal distance between the gangue deposition position and the hydraulic support, m.

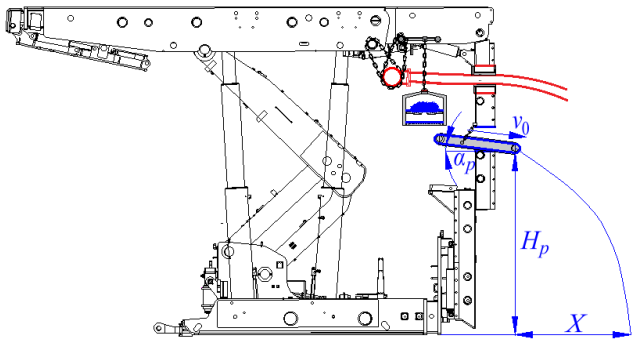


Figure 6. Schematic diagram of gangue throwing by belt conveyor behind the support.

The relationship among these parameters can be expressed as follows:

$$\begin{cases} H_p = v_0 \sin \alpha_p + \frac{1}{2} g t^2 \\ X = v_0 \cos \alpha_p \end{cases} \tag{10}$$

where g denotes the gravitational acceleration, 9.8 m/s^2.

Combining the above equations, the following relationship is derived:

$$H_p = v_0 \sin \alpha_p + \frac{1}{2} g \frac{X^2}{(v_0 \cos \alpha_p)^2} \tag{11}$$

The thrown gangue particles should fall within the backfilling space and avoid collision with the rear backfilled body. Therefore, the allowable range of X is from zero to the width of the backfilling space.

3. Additional Resistance Caused by Misalignment of the Suspended Belt Support Frame

The rear belt system of the hydraulic support is connected by a fully rigid structure and consists of multiple suspended belt support frames. The misalignment of the belt support frames is mainly caused by the following two aspects: ① misalignment resulting from assembly errors or dimensional deviations of the components; ② misalignment of the suspended support frames caused by displacement or misalignment of the hydraulic supports.

Due to the misalignment of the suspended belt support frames behind the hydraulic support, the suspended gangue-throwing belt conveyor may experience frictional collision and mechanical interference with the support frames during operation. Since the suspended gangue-throwing belt conveyor is driven by an electric motor, such interference increases the resistance during transportation and results in additional power consumption, as shown in Figure 7.

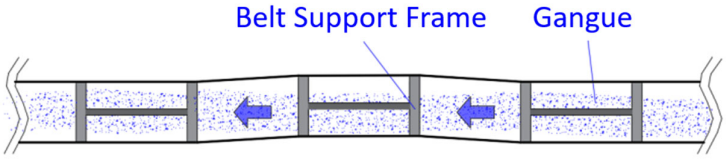


Figure 7. Schematic diagram of hanging misalignment for the belt conveyor frame.

When the misalignment is severe, belt deviation and belt jamming may occur, which can further lead to motor failure. Moreover, frictional collisions caused by frame misalignment may result in gangue spillage from the belt conveyor, posing potential safety risks to workers below. Therefore, the misalignment of the belt suspension frames negatively affects the driving system, load-bearing system, and personnel safety.

In practical applications, belt suspension frames with the same specifications should be preferentially adopted, and the hydraulic supports should be maintained in a straight alignment state as much as possible.

The transportation resistance F_{H} of the suspended gangue-throwing belt conveyor is calculated using Equation (12). Considering the misalignment of the belt suspension frames, an additional resistance coefficient C_{N} is introduced, whose value is determined according to the degree of belt frame misalignment.

$$F_H = C_N \mu_0 l_{pd} g\left[q_t + (2q_B + q_{pd})\cos\beta\right] + F_N \tag{12}$$

where μ_0 is the simulated friction coefficient; l_{pd} is the length of the suspended belt conveyor, m; q_{t} is the rotating mass per unit length of the carrying and return idler sets, kg/m; q_{B} is the mass per unit length of the conveyor belt, kg/m; β is the inclination angle of the conveyor in the conveying direction, °; and F_{N} is the remaining additional resistance, N.

Based on Equation (12), the maximum allowable transportation resistance $F_{\mathrm{H\,max}}$ determined by the motor power can be calculated as follows:

$$F_{H\max} = \frac{1000\eta\xi \cdot \xi_d N}{v_{pd} K_d} \tag{13}$$

where η denotes the transmission efficiency of the motor; ξ represents the voltage drop coefficient; ξ_{d} denotes the power imbalance coefficient; q_{B} represents the mass per unit length of the conveyor belt, kg/m; N denotes the motor power, kW; and K_{d} represents the power reserve coefficient.

4. Engineering Case and Design Verification of a Large-Height Paste–Solid Composite Backfilling Hydraulic Support

4.1. Engineering Background

The Pingdingshan mining area contains approximately 1.8 billion tons of coal resources affected by the "three-under" mining conditions (coal resources beneath buildings, water bodies, and railways). The western mining section of Pingmei No. 11 Coal Mine is affected by surface structures, including roads and villages, resulting in a large amount of high-quality idle coal resources being difficult to recover. Meanwhile, a large quantity of coal gangue solid waste generated during coal production is difficult to dispose of effectively. Based on the development of backfilling mining technology, Pingmei No. 11 Coal Mine initiated a research project on composite backfilling mining behind composite roof supports. The first backfilling working face, namely the No. Ji16-17-24100 working face, was established to explore solutions for the recovery of coal resources constrained by surface structures. The layout of the backfilling working face is shown in Figure 8. For the Ji16-17-24100 working face, the mining length is 261 m and the strike length is 970 m. The average mining height is 6.0 m, and the average coal-seam dip angle is 13°. These are average values for the working face and are distinct from the zonal inclination values used in the spatial-compatibility calculations. The coal-seam thickness ranges from 3.3 to 6.2 m.

The recoverable coal reserves of the working face reach 1.7 million tons.

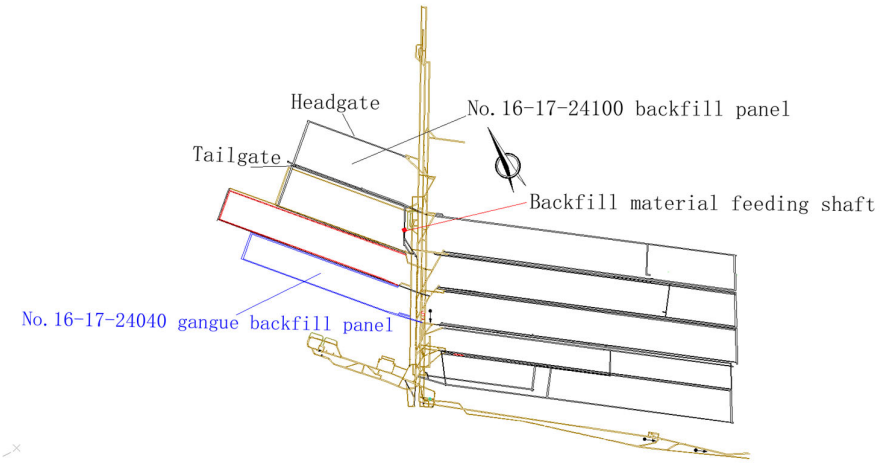


Figure 8. Backfill face layout diagram of Pingmei No. 11 Coal Mine.

4.2. Determination of Key Parameters and Selection Design of the Hydraulic Support

The large-height paste–solid composite backfilling hydraulic support is one of the major pieces of equipment used in the working face. It is applied together with the shearer, scraper conveyor, and multi-hole bottom-unloading scraper conveyor. The support plays a key role in roof control, surrounding-rock isolation, and maintenance of the working space. In combination with the scraper conveyor, the hydraulic support can advance automatically, thereby enabling continuous operation of the mining face.

The basic design principles of the backfilling hydraulic support are as follows: under the backfilling mining method, the design of the hydraulic support should satisfy the fundamental requirements of the backfilling process. The determination of support strength should consider the basic conditions of the coal seam and the characteristics of strata pressure behavior at the working face. The designed hydraulic support should meet the ventilation requirements of the mining face to ensure effective airflow. In addition, the backfilling hydraulic support should be compatible with the operating requirements of min-

ing equipment, such as the shearer and scraper conveyor. The design of the main backfilling mechanism should also satisfy the functional requirements of the backfilling operation.

1. Design of Support Height

To ensure the normal operation of the hydraulic support columns, the maximum structural height of the support is generally designed to be 200–300 mm higher than the maximum mining height, while the minimum structural height should be 250–350 mm lower than the minimum mining height. Considering the thickness range of the Ji coal seam (3.3–6.2 m), the structural height of the hydraulic support was determined to be 3.0–6.5 m.

2. Determination of Support Strength

The support strength is generally determined according to the geological conditions of the coal seam and roof strata. The calculation equation is expressed as follows:

$$q = KM\rho g \times 10^3 \quad (14)$$

In the support-strength calculation, K is the roof-thickness coefficient and is taken as 5 based on the design standard. The roof-rock density ϱ_r is taken as 25×10^3 kg/m^3 based on the geological report.

Accordingly, the required support strength of the hydraulic support is calculated as 0.81 MPa. According to the working characteristic curve of the hydraulic support, when the support enters the constant-resistance stage, the resistance acting on the support corresponds to the working resistance. Considering the roof beam area, the calculated working resistance is 11,809.8 kN. Considering the arrangement of four hydraulic columns, the designed working resistance of the support is determined as 13,000 kN, which satisfies the requirements for roof control.

3. Determination of Support Spacing

The support spacing refers to the center-to-center distance between two adjacent backfilling hydraulic supports arranged in the mining face. This spacing is related to the support type and the scraper conveyor. The advancing cylinders of the backfilling hydraulic supports are connected to each middle trough section of the scraper conveyor, enabling mutual support and continuous advancement of the fully mechanized mining equipment toward the new working area. Therefore, the support spacing is mainly determined by the length of the middle trough section of the scraper conveyor. The mine plans to use the existing SGZ1000/2 × 1000 scraper conveyor (SANY Heavy Equipment Co., Ltd., Pune, Maharashtra, India), whose middle trough section has a length of 1.75 m. Therefore, the support spacing of the backfilling hydraulic support is determined to be 1.75 m.

Accordingly, the ZC13000/30/65D backfilling hydraulic support was selected for the Ji16-17-24100 working face; its key technical parameters are listed in Table 1.

Table 1. Main technical parameters of ZC13000/30/65D backfilling hydraulic support.

Parameter	Value	Parameter	Value
Support height	3000–6500 mm	Advancing step	800 mm
Center distance	1750 mm	Applicable inclination angle	≤15°
Initial support force	10,112 kN	Pump station pressure	37.5 MPa
Working resistance	13,000 kN	Control mode	Electro-hydraulic control
Support strength	0.96–1.03 MPa	Designed weight	53.5 ± 3%

4.3. Design and Selection of Newly Added Support Structures

To satisfy the requirements of paste–solid composite backfilling, the backfilling hydraulic support requires the addition of a suspended gangue-throwing belt conveyor and a

side-throwing belt conveyor based on the original mechanical structure. The selection and design of these newly added structures were carried out accordingly.

1. Structural Design of the Suspended Gangue-Throwing Belt Conveyor

The suspended gangue-throwing belt conveyor mounted on the rear roof beam of the hydraulic support is mainly used for transporting gangue required for backfilling. To improve its adaptability to variations in the working face inclination and the dynamic displacement caused by support advancing, the steel-frame belt structure adopts a modular design, and multi-degree-of-freedom adjustment is achieved through hinged suspension connections. To enhance the adaptability of the belt conveyor under different working face inclination conditions and support advancing operations, the belt conveyor is independently fixed to the roof beam of each individual hydraulic support. A wear-resistant belt with high mechanical strength and flame-retardant and antistatic properties was selected. The independent fixation of the belt on each support roof beam avoids stress concentration caused by the coordinated movement of multiple supports and reduces the risk of belt deviation. In addition, guide idlers are installed beneath the belt to further reduce operational resistance and improve transportation efficiency. The detailed structure is shown in Figure 9, and the key technical parameters are listed in Table 2.

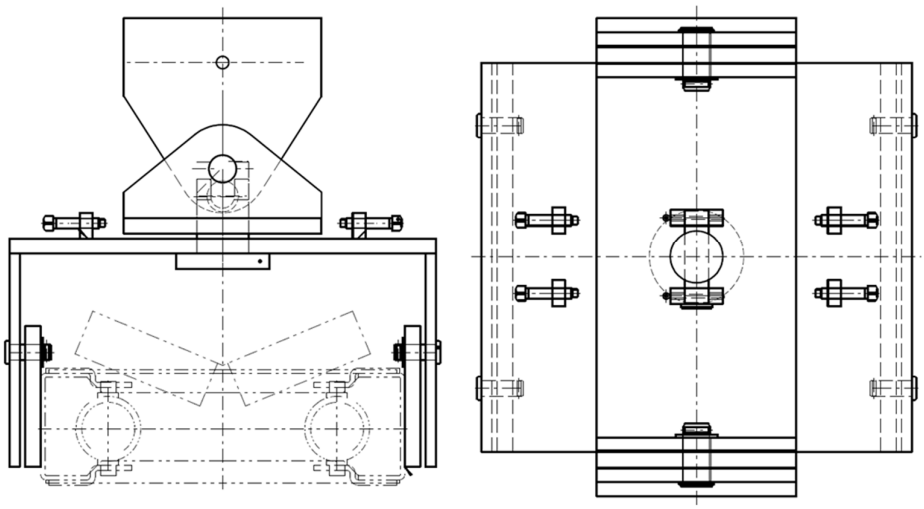


Figure 9. Structural diagram of suspended gangue dumping belt conveyor.

Table 2. Main technical parameters of the suspended gangue dumping belt conveyor.

Parameter	Value
Conveying capacity	100 t/h
Belt speed	3 m/s
Belt width	600 mm
Conveyor belt model	PVG800S
Hydraulic motor model	GM46009GD40

2. Structural Design of the Side-Throwing Belt Conveyor

The primary function of the gangue-throwing belt, located on the isolation baffle of the backfilling hydraulic support, is to hurl the gangue transported by the suspended belt conveyor into the filling space. To minimize gangue loss when it transfers from the suspended belt to the throwing belt and to prevent accumulation in front of the isolation baffle, a baffle is installed along the throwing direction. To ensure the smooth implementation of the combined gangue-paste backfilling, a throwing port is opened on the upper isolation

baffle for gangue discharge. The entire side-throwing belt is fixed to the upper structure via hinges, and an adjustable-angle baffle is employed to control the trajectory of the discharged gangue. Furthermore, to enhance the throwing velocity of the side-throwing belt, a compact hydraulic motor is installed on the side close to the suspended throwing belt, achieving a belt speed of 3.5 m/s. Figure 10 shows the side-throwing belt conveyor.

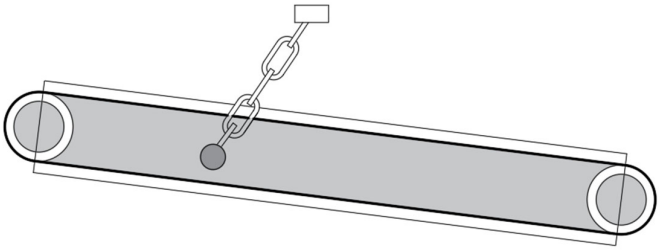


Figure 10. Structural diagram of side-throwing belt conveyor.

5. Case Study and Design Verification of Hydraulic Support Operational Characteristics

This case study presents a design-stage engineering adaptability assessment of the ZC13000/30/65D paste–solid composite backfilling hydraulic support for the Ji16-17-24100 working face at Pingmei No. 11 Coal Mine. The six characteristic categories are assessed using structural design information, analytical calculations, and equipment selection parameters. The assessment methods and evidence reported for the six characteristic categories are summarized in Table 3.

Table 3. Summary of assessment methods, results, and limitations.

Characteristic Category	Assessment Method	Results Reported in This Study	Scope and Limitations
Structural	Review of the support configuration and design parameters (Sections 2.1 and 4.3; Tables 1 and 2).	The support incorporates suspended gangue-throwing and side-throwing belt conveyors. Its working height is 3.0~6.5 m, and its rated working resistance is 13,000 kN.	Based on the reported design information; no separate quantitative structural-performance test is reported.
Support	Support-strength and working-resistance calculations using the methods in Section 5.1.	Table 4 reports working-resistance ranges of 7858.54~11,784.85 kN, 8425.86~11,308.40 kN, 3781.82~4295.52 kN, and 3574.52~4057.06 kN.	Design-stage calculations; field measurements of working resistance are not reported.
Load-bearing	Force and moment equilibrium calculations under seven canopy-load patterns.	The calculated front-to-rear leg-load ratios range from 1:0.0761 to 1:13.1534.	The analysis compares load patterns; individual leg loads, leg-capacity checks, and allowable eccentricity are not reported.
Sealing	Assessment against the baffle-overlap and contact-angle criteria in Section 3.1.	The baffle structure and theoretical sealing criteria are described.	Case-specific overlap and contact-angle results, as well as leakage measurements, are not reported.
Spatial compatibility	Geometric compatibility calculations for the support, paste pipeline, suspended belt conveyor, and isolation baffle (Table 6).	Geometric check results are reported for the specified working-face conditions.	Design-stage assessment; field interference measurements are not reported.
Backfilling coordination	Calculation of side-throwing belt speed and suspended-belt conveying resistance (Tables 7 and 8).	The selected side-throwing belt speed is 3.5 m/s, within the calculated range of 0~5.48 m/s. The reported maximum allowable resistance of the suspended belt is 33,640 N.	Design-stage calculations; field measurements of conveying resistance, filling rate, and filling ratio are not reported.

5.1. Check of Support Characteristics of the Powered Support

The support characteristics of the backfilling hydraulic support were evaluated and checked using four methods: the caved-zone-height strata weight method, the 6~8 times mining height rock heavy stress method, the detached roof block method, and the collaborative roof-control calculation method involving the coal wall, the backfilling powered support, and the backfill body. The first three methods are relatively conventional and do not account for the influence of the backfill body on the working resistance; therefore, their calculation processes are omitted here.

The core of determining the working resistance of the backfilling hydraulic support using the collaborative roof-control calculation method (involving the coal wall, the backfilling powered support, and the backfill body) lies in constructing and solving a ternary collaborative roof-control mechanical model. This model integrates the movement and control characteristics of the overlying strata in backfill mining, the overall movement mechanical model of the overlying strata, and the mechanical model of the canopy of the support. During the solution process, the roof load of the working face and the load pattern on the support canopy are derived through the overall movement mechanical model of the overlying strata and the canopy mechanical model. Specifically, based on the mining-geological conditions and the movement and control characteristics of the overlying strata in backfill mining, the overall movement mechanical model of the overlying strata is established. Next, the critical filling ratio corresponding to different breaking states of the overlying strata is solved. Then, the target filling ratio is designed according to the filling objectives and the load-bearing compression characteristics of the backfilling materials, and is compared with the critical filling ratio to determine the magnitude of the roof load at the working face based on the breaking state of the overlying strata.

The calculation is performed assuming that the canopy is subjected to a triangular linear load, as illustrated in Figure 11.

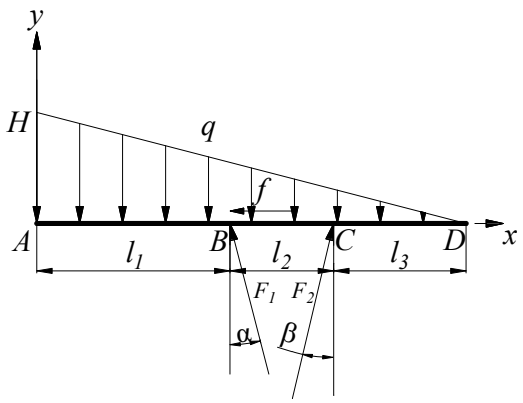


Figure 11. Schematic diagram of the beam under a triangular linear load.

The load pattern of the canopy subjected to an inverted triangular linear load is expressed as

$$q(x) = -\frac{qx}{l_1 + l_2 + l_3} + q \tag{15}$$

Substituting the data for calculation, the working resistance of the backfilling powered support ranges from 3574.52~4057.06 kN, with a support strength of 0.56~0.67.

Finally, the working resistances are calculated using the detached roof block method, the estimated weight method of caved-zone roof rocks, the estimated weight method of caved-zone rocks considering the fracture angle, and the collaborative roof-control calculation method involving the coal wall, the backfilling powered support, and the backfill body. The maximum value among these calculations is adopted as the actual working resistance

for the selection of the backfilling hydraulic support. The specific verification of the support characteristics is presented in Table 4, which indicates that the ZC13000/30/65D four-leg backfilling powered support fully meets the requirements for support characteristics.

Table 4. Verification results table of support characteristics.

Calculation Method	Support Strength/MPa	Working Resistance/kN	Initial Supporting Force/kN
Strata weight method based on caved zone height	0.62~0.93	7858.54~11,784.85	7070.91~9427.88
Rock overburden stress method for 6~8 times mining height	0.76~1.02	8425.86~11,308.40	6785.04~9046.72
Detached roof block method	0.63~0.72	3781.82~4295.52	3025.46~3436.42
Coal wall—backfilling hydraulic support–backfill body collaborative roof control method	0.56~0.67	3574.52~4057.06	2859.62~3245.65
Parameters of ZC13000/30/65D support	0.96–1.03	13,000	10,112
Verification results	Conforming	Conforming	Conforming

5.2. Verification of Load-Bearing Characteristics

The load on the backfilling hydraulic support is generally lower than that on conventional working faces. However, due to the interaction between the support and the surrounding rock, which affects the roof-control performance, the support structure and its support characteristics must conform to the movement laws of the overlying strata in the coal mining face. The load distribution on the canopy under different overburden load patterns, as well as the stress state of the legs, form the basis for studying the support–rock interaction.

As the geological conditions of the working face change continuously, the support status and its contact state with the roof vary over time, leading to real-time variations in the overburden load. In practice, it is difficult to determine the exact load pattern during a specific study. Therefore, it is necessary to first define the overburden load patterns and the support modes of the backfilling hydraulic support. For the four-leg backfilling hydraulic support, based on both ideal and non-ideal engineering conditions, seven load patterns acting on the canopy are established: uniformly distributed load, positive triangular linear load, inverted triangular linear load, right-convex curve load, left-convex curve load, right-concave curve load, and left-concave curve load [27].

For the multiple support load patterns, the load equations for the front and rear canopies under different patterns are formulated. Furthermore, the force and moment equilibrium equations for the support in a balanced state are derived. Using the dimensions of the ZC13000/30/65D support used at the Ji16-17-24100 working face (l_1 = 3.496 m, l_2 = 2.019 m, l_3 = 2.583 m, $\alpha = 3°$, $\beta = 4°$; Figure 11), the equilibrium equations are solved for the front-to-rear leg load ratio under each of the seven load patterns. The results are listed in Table 5.

The front-to-rear leg load ratios in Table 5 are analytical results obtained from force and moment equilibrium calculations for seven prescribed canopy-load patterns. The ratio of 1:13.1534 corresponds to the left-concave load pattern and represents an extreme theoretical load-distribution case within the adopted model. It is included to examine the sensitivity of the leg-load distribution to the assumed canopy-load pattern; it is not a measured operating load or a representation of the normal loading condition.

Table 5. Load ratio under different loading configurations.

Load Pattern	Front-to-Rear Leg Load Ratio F_1/F_2	Remarks
Uniformly distributed load	F_1:F_2 = 1:1.0341	Ideal condition
Positive triangular linear load	F_1:F_2 = 1:0.1786	-
Inverted triangular linear load	F_1:F_2 = 1:9.8425	-
Right-convex curve load	F_1:F_2 = 1:0.5376	-
Left-convex curve load	F_1:F_2 = 1:3.3158	-
Right-concave curve load	F_1:F_2 = 1:0.0761	Extreme condition
Left-concave curve load	F_1:F_2 = 1:13.1534	Extreme condition

5.3. Verification of Support Spatial Compatibility

Based on the actual geological conditions of the Ji16-17-24100 backfilling working face, the working face was divided into zones along the strike direction and along the dip direction at the open-off cut. The zoning scheme is shown in Figure 12. Using the formulas presented in Section 3.2, the verification results of the support spatial compatibility under the actual geological conditions of the backfilling working face are summarized in Table 6.

For the strike-direction zoning, the inclination angle is signed according to the mining direction: positive values indicate up-dip sections, negative values indicate down-dip sections, and 0° indicates a nearly horizontal section. The listed values are zonal values used in the geometric calculations and are distinct from the average coal-seam dip angle of 13° reported for the entire working face.

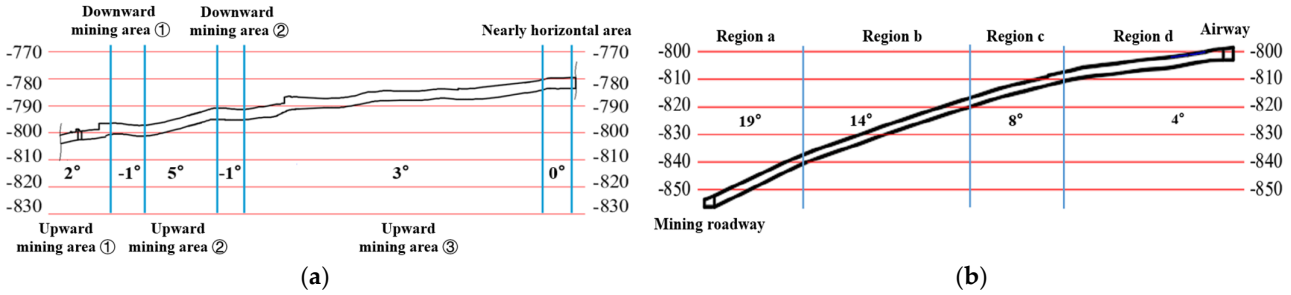


Figure 12. Working face area division: (**a**) Zoning of the working face along the strike direction. (**b**) Dip-direction zoning of the working face at the open-off cut.

Table 6. Verification results of spatial compatibility.

Direction	Region	Working Face Inclination/(°)	D_1/(mm)	D_2/(mm)	χ/(mm)	Verification Result
Strike	Up-dip mining section ①	2	421.37	69.41	495.63	Pass
	Down-dip mining section ①	−1	489.99	118.22	452.85	Pass
	Up-dip mining section ②	5	331.68	20.07	554.11	Pass
	Down-dip mining section ②	−1	489.99	118.22	452.85	Pass
	Up-dip mining section ③	3	398.74	53.02	510.11	Pass
	Nearly horizontal section	0	467.00	77.02	467.00	Pass
Dip	Region a	19	467.00	25.56	467.00	Pass
	Region b	14	467.00	49.29	467.00	Pass
	Region c	8	467.00	68.42	467.00	Pass
	Region d	4	467.00	77.56	467.00	Pass

In addition, the working state of the backfilling hydraulic support varies with the coal seam thickness. The suitable mining height for the composite backfilling hydraulic support ranges from 3.0 to 6.5 m. A sudden increase or decrease in coal seam thickness

can significantly affect the motion of the support canopy, which in turn influences the rear sealing plate of the support. As a result, interference of the sealing plate may occur.

Moreover, when the roof condition is poor, premature roof breakage may take place, leading to an increased load on the support and considerable subsidence of the rear canopy at the hinge point. Consequently, the front and rear canopies become uneven, and the rear canopy subsides. As the rear canopy subsides, the clearance to the suspended gangue-throwing belt decreases, increasing the risk of interference.

5.4. Verification of Backfilling-Coordination Characteristics

Based on the actual geological conditions of the Pingmei No. 11 Mine, the backfilling-space width is 4 m, the side-throwing belt discharge angle is α_p, and the belt installation height H_p is 3.6 m. The calculated side-throwing belt speeds are presented in Table 7.

Table 7. Verification results of speed of side-throwing belt conveyor.

Region	X (m)	V (m/s)
All regions of the working face	1	1.22
All regions of the working face	2	2.53
All regions of the working face	3	3.81
All regions of the working face	4	5.48

Using these values, an initial velocity of 0~5.48 m/s satisfies the gangue-discharge requirements of the working face. The selected side-throwing belt speed is 3.5 m/s, which falls within the range of 0–5.48 m/s; therefore, the verification result is acceptable.

Meanwhile, the calculated maximum allowable haulage resistance of the suspended gangue-throwing belt conveyor is $F_{H\,max}$ = 33,640 N. Under normal operating conditions, the haulage resistance of the suspended gangue-throwing belt conveyor should remain below this limit. As shown in Figure 12b, verifications were conducted for four zones along the dip direction of the working face, and the results are presented in Table 8.

Table 8. Verification results of resistance of suspended throw belt conveyor.

Region	Strike Inclination/(°)	Additional Resistance Coefficient C_N	Transportation Resistance F_H/(N)	Verification Status
Region a	19	1.0	697.23	19
Region b	14	1.1	2073.64	14
Region c	8	1.5	2842.23	8
Region d	4	1.73	4148.94	4

The design-stage calculations indicate that the selected support and the associated belt-conveying arrangements satisfy the specified support-capacity, spatial-clearance, and backfilling-coordination criteria under the stated engineering conditions. Future work will monitor support working resistance, suspended-belt conveying resistance, backfilling rate, and leakage at the isolation baffle during field operation. The measured data will be used to compare the design-stage predictions with actual operating performance and to refine the assessment criteria.

6. Conclusions

1. An operational-characteristics evaluation framework for the paste–solid composite backfilling hydraulic support was established. Six categories—structural, support, load-bearing, sealing, spatial-compatibility, and backfilling-coordination characteristics—

were defined, and corresponding verification methods were proposed, providing a theoretical basis for support design and engineering application.
2. Quantitative criteria and calculation procedures were formulated for sealing, spatial compatibility, and backfilling coordination. These procedures provide design-stage checks for the specified support geometry and operating conditions.
3. For the Ji16-17-24100 working face at Pingmei No. 11 Coal Mine, the design-stage assessment supports the selection of the ZC13000/30/65D support with a rated working resistance of 13,000 kN. The selected side-throwing belt speed of 3.5 m/s lies within the calculated admissible range of 0–5.48 m/s, and the calculated maximum allowable conveying resistance of the suspended belt is 33,640 N. These results indicate that the selected design parameters meet the stated calculation criteria under the specified conditions; they are design-stage checks and do not constitute field-operation validation.

Author Contributions: Conceptualization, G.Z.; methodology, G.Z.; software, M.L.; validation, M.L.; formal analysis, M.L.; investigation, Q.Z.; resources, Q.Z.; data curation, Z.J.; writing—original draft preparation, Z.J.; writing—review and editing, R.Z.; visualization, T.H.; supervision, Z.J.; project administration, Y.Z.; funding acquisition, G.Z. All authors have read and agreed to the published version of the manuscript.

Funding: This research was supported by the "7+2" Major Strategic Scientific Research Project of China Pingmei Shenma Holding Group Co., Ltd., under the project title "Key Technologies and Engineering Demonstration of Paste-Bulk Synergistic Backfilling of Coal-Based Solid Waste in Kilometer-Deep Shafts with Composite Roofs and Large Mining Height" (grant number 4104022024110201).

Data Availability Statement: The data presented in this study are available on request from the corresponding author.

Conflicts of Interest: Guochuan Zhang, Mao Li and Tairan Han received funding from China Pingmei Shenma Holding Group Co., Ltd. Yuanzhi Zhang is employed by Pingdingshan Tianan Coal Industry Co., Ltd. The funding sponsors had no role in the design of the study; in the collection, analyses, or interpretation of data; in the writing of the manuscript, and in the decision to publish the results.

References

1. Ge, S.R.; Liu, S.Q.; Liu, J.C.; Wang, B.; An, X.Y.; Xiang, L. Effectiveness of Secure Supply and Carbon Reduction in the Coal Sector for Strengthening the Energy Power of China. *Strateg. Study CAE* **2024**, *26*, 40–51. [CrossRef]
2. Liu, F.; Guo, L.F.; Zhang, J.M.; Wang, L. Synergistic Mode of Digitalization-Intelligentization-Greeniation of the Coal Industry and Its Path of Building New Coal Productivity. *J. China Coal Soc.* **2024**, *49*, 1–15.
3. Xie, H.P.; Qian, M.G.; Peng, S.P.; Hu, S.S.; Cheng, Y.Q.; Zhou, H.W. Sustainable Capacity of Coal Mining and Its Strategic Plan. *Strateg. Study CAE* **2011**, *13*, 44–50.
4. Zhang, J.X.; Zhang, Q.; Zhou, N.; Li, M.; Huang, P.; Li, B.Y. Research Progress and Prospect of Coal-Based Solid Waste Backfilling Mining Technology. *J. China Coal Soc.* **2022**, *47*, 4167–4181.
5. Qian, M.G.; Miao, X.X.; Xu, J.L. Green Mining of Coal Resources Harmonizing with Environment. *J. China Coal Soc.* **2007**, *32*, 1–7.
6. Qian, M.G.; Miao, X.X.; Xu, J.L.; Cao, S.G. On Scientized Mining. *J. Min. Saf. Eng.* **2008**, *25*, 1–10. [CrossRef]
7. Miao, X.X.; Qian, M.G. Research on Green Mining of Coal Resources in China: Current Status and Future Prospects. *J. Min. Saf. Eng.* **2009**, *26*, 1–14.
8. Xie, H.P.; Zhang, J.X.; Gao, F.; Li, B.Y.; Li, C.B.; Xie, Y.C.; Zhou, N. Theory and Technical Conception of Carbon-Negative and High-Efficient Backfill Mining in Coal Mines. *J. China Coal Soc.* **2024**, *49*, 36–46.
9. Zhang, J.X.; Zhang, Q.; Zhou, N.; Li, M.; Ju, F. Innovation and Practice of Quadrilateral Development Model for Coal Resources. *J. China Coal Soc.* **2025**, *50*, 2020–2036.
10. Zhang, Q.; Zhang, J.X.; Yang, K.; Ju, F.; Huang, P.; Wang, Y.B.; Lv, H.N. Research on Technical Conception and Theoretical Framework of Fully Mechanized Top-Coal Caving Backfill Mining. *J. China Univ. Min. Technol.* **2024**, *53*, 469–482.
11. Zhang, Q.; Cui, P.F.; Zhang, J.X.; Wang, Y.B.; Yang, J.H.; Zong, T.C.; Bai, Y.; Jin, Z.S.; Feng, J.Y.; Zhu, X.H. Three-Dimensional Backfilling Mining Method and Engineering Practice in Coal Mine. *J. China Coal Soc.* **2026**, *51*, 966–976.

12. Zhu, M.B.; Liu, L.; Wang, S.M.; Wei, B.N.; Rong, R.Y.; Zhang, W.Z.; Zhuang, D.D.; Jia, Q.F. Backfill-Strip Mining and CO_2 Mineralization Sequestration in Coal Mine Goaves: A Synergetic Method and Its Key Technologies. *Coal Geol. Explor.* **2025**, *53*, 143–155.
13. Zhang, Z.Y.; Zhang, J.X.; Zhou, N.; Song, Y.Z.; Cheng, G.; Liu, N.N.; Yan, R.B.; Sun, D.S. Study on Impermeability of Fly Ash Sand-Based Sealing Wall under CO_2 Gas Storage in Strip Backfilling Goaf. *J. China Coal Soc.* **2025**, *50*, 2922–2939.
14. Deng, X.J.; Liu, H.; Zhang, J.X.; Zhao, Y.L.; Li, Y.; Bian, L.G.; Tian, X.G.; Xie, J. Study on Microbial Cemented Backfill Mining Technology. *J. Min. Sci. Technol.* **2023**, *8*, 439–451.
15. Zhang, J.X.; Wang, J.Y.; Zhou, N.; Kong, Y.L.; Zhu, C.L.; Liu, H.F. Collaborative Mining System of Geothermal Energy and Coal Resources in Deep Mines. *Chin. J. Eng.* **2022**, *44*, 1682–1693.
16. Li, B.Y.; Zhang, J.X.; Liu, H.F.; Zhou, N.; Yan, H.; Li, M. Energy-Stored Backfilling Technology and Energy Storage Efficiency Enhancement Mechanism in Coal Mine Goaf. *J. Min. Saf. Eng.* **2022**, *39*, 1161–1168.
17. Zhang, J.X.; Liu, H.F.; Zhou, N.; Yan, H.; Li, B.Y. Design and Technical System of Phase Change Heat Storage and Mine Geothermal Exploiting Method of Functional Backfilling in Deep Mine. *J. Min. Saf. Eng.* **2023**, *40*, 933–944.
18. Yang, K.; Yu, X.; He, X.; Zhao, X.Y.; Fang, J.J.; Wei, Z.; He, S.X. Method and Application of Coal-Based Solid Waste Filling in Multi-Layer Three-Dimensional Space of Coal Mining. *Coal Sci. Technol.* **2025**, *53*, 46–64.
19. Lyu, C.; Lyu, W.Y.; Sun, Q.; Xie, P.S.; Lang, D.; Ji, S.T.; Hu, J.J. Theoretical and Technical Concept of Cemented Backfill Material for Flexible Enhanced Thermal Energy Storage in Coal Underground Space. *Coal Sci. Technol.* **2025**, *53*, 104–113.
20. Chang, Q.L.; Gao, L.; Fang, J.G.; Zhang, B.; Sun, C.; Hu, P. Collaborative Load-Bearing Mechanism between the Filling Body and the Surrounding Rock in Multi-Layer Mining of Thick Coal Seams in Deep Mines. *J. Min. Saf. Eng.* **2025**, *42*, 510–520.
21. Liu, J.G.; Zhao, J.W.; Liu, Y.; Yang, J.H.; Shi, Y.N.; Wang, Y.Y.; Chen, F. General-Purpose Expansion Type Solid Modification Backfilling Mining Technology and Equipment for Coal Mines. *J. China Coal Soc.* **2024**, *49*, 380–399.
22. Wang, S.S.; Yang, R.S.; Li, Y.L.; Yue, Z.W. Study on Mechanical Properties and Failure Characteristics of Aeolian Sand Cemented Backfill. *J. Min. Saf. Eng.* **2025**, *42*, 418–429. [CrossRef]
23. Li, M.; Wang, Z.H.; Sun, W.C.; Wu, C.; Sun, S.; Cao, P.; Sun, C. Support-Rock Interaction and Supporting Parameter Optimization in Deep Backfilling Longwall Faces with Hard Roof. *Chin. J. Rock Mech. Eng.* **2024**, *43*, 2753–2765.
24. Sun, X.G.; Zhou, H.Q.; Zhao, L. Research on Paste and Solid Collaborative Fully Mechanized Mining Filling Technology. *Shandong Coal Sci. Technol.* **2025**, *43*, 173–177.
25. Zhang, Q.; Du, C.L.; Zhang, J.X.; Wang, J.Q.; Li, M.; Qi, W.Y. Backfill Support's Backfill and Operation Properties and Evaluation. *J. Cent. South Univ.* **2018**, *25*, 1524–1534. [CrossRef]
26. Zhang, Q.; Wu, Z.Y.; Du, E.B.; Chen, Y.; Huang, P.; Li, M. Working Resistance Design Method of Backfilling Shield. *J. Min. Saf. Eng.* **2020**, *37*, 118–127.
27. Zhang, Q. Roof Control Mechanism by Coordination with Backfilled Body and Backfill Support in Solid Backfill Mining Technology. Ph.D. Thesis, China University of Mining and Technology, Xuzhou, China, 2015.

Disclaimer/Publisher's Note: The statements, opinions and data contained in all publications are solely those of the individual author(s) and contributor(s) and not of MDPI and/or the editor(s). MDPI and/or the editor(s) disclaim responsibility for any injury to people or property resulting from any ideas, methods, instructions or products referred to in the content.